Geophys. J. Int. (2006) **165,** 516–526 doi: 10.1111/j.1365-246X.2006.02858.x

Comparison of frequency of occurrence of earthquakes with slip rates from long-term seismicity data: the cases of Gulf of Corinth, Sea of Marmara and Dead Sea Fault Zone

N. N. Ambraseys

Department of Civil and Environmental Engineering, Imperial College, London SW7 2BU*, UK. E-mail: n.ambraseys@imperial.ac.uk*

Accepted 2005 November 3. Received 2005 September 14; in original form 2005 March 24

SUMMARY

In this article, through the comparison of knowledge relating to historical earthquakes with the understanding of present-day earthquake mechanics and overall GPS slip rates in the eastern Mediterranean region, it has been possible to obtain an idea of how frequently large earthquakes may be expected in some parts of the region. It has also been possible to make an assessment from these early events of slip rates over a long period of time for the Gulf of Corinth in Greece, the Marmara Sea in Turkey and the Dead Sea Fault System, as well as deriving long-term magnitude–frequency relations for these same regions.

It has been demonstrated that slip rates calculated from historical data are in general comparable to those calculated from GPS measurements and field observations, while the size of historical earthquakes and their uncertainty can be quantified. This permits a more reliable estimation of the long-term hazard, the calculation of which is the concern of the engineering seismologist. It has also been shown that in most cases large earthquakes are less frequent when they are estimated from long-term data sets rather than from the instrumental period making the notion of recurrence time and of hazard assessment, questionable.

This study focuses on some of the few areas in the world for which long-term macroseism information exists and which facilitate this kind of analysis.

Key words: Dead Sea Fault Zone, earthquakes, Gulf of Corinth, historical seismicity, slip rates, Sea of Marmara.

INTRODUCTION

Recent earthquakes in the Eastern Mediterranean region, which has a long and well-documented historical record, suggest that the seismicity record of the 20th century covers too short a time span and is, therefore, not a useful guide to estimating long-term earthquake activity. This raises a number of questions, which are addressed here:

(1) Is the level of uncertainty of the location, and in particular the magnitude of historical earthquakes, insignificant enough to allow this information to be useful for the estimation of long-term hazard and strain rates?

(2) Is this new information, which is based on macroseismic data, consistent with what is known about earthquake mechanics today and does it contribute to a better understanding of earthquake hazard?

The object of this article is to investigate these questions using the results from the reappraisal of the long-term seismicity of the Gulf of Corinth in Greece, of the Marmara Sea in Turkey and of the of Dead Sea Fault System, which runs through Syria, Lebanon, Israel and Jordan.

The motivation here is to see whether the use of new and improved databases, chiefly of historical information, but also of recent results from GPS measurements and models, and of field measurements, would confirm general conclusions drawn earlier, which were based on historical seismicity. In other words, that it is not advisable to ignore the chance that much, or all, of our seismic records of the last 100 yr may result from a quiescent or energetic period in seismic activity, nor to make assumptions based on incomplete data sets.

Data

The threestudy regions, which are of different dimensions and style of faulting, are shown in Fig. 1, and their dimension and seismologic characteristics are summarized in Table 1.

The long-term seismicity of the Gulf of Corinth in Greece since 1697, and of the Marmara Sea region in Turkey since the beginning of our era, has already been dealt with by Ambraseys & Jackson (1997, 2000), and the revised database used in this work can be found in Meghraoui (2004–5a). Table 2 lists the earthquakes of $M_S >$ 7.0 identified in these three study areas. However, some remarks on

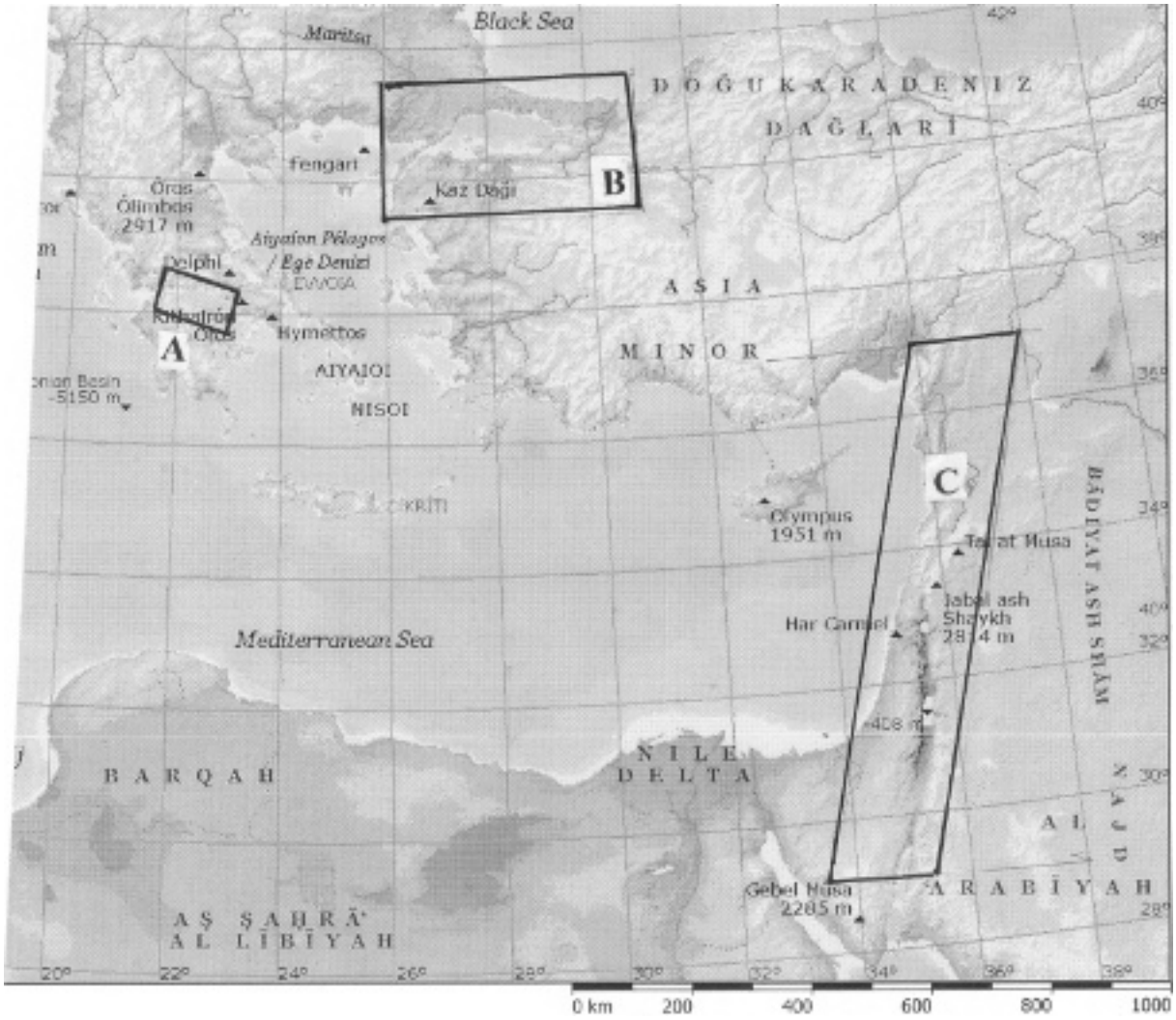

Figure 1. Location map. C = Gulf of Corinth, M = Sea of Marmara, D = Dead Sea Fault Zone.

the method used to estimate recurrence frequencies and slip rates may be in order.

Magnitude assessment

Surface wave magnitudes M_{Si} of pre-1896 earthquakes were calculated from intensity data using the scaling formula,

$$M_{\mathrm{Si}} = -1.54 + 0.65(I_{\mathrm{i}}) + 0.0029(r_{\mathrm{i}}) + 2.14\log(r_{\mathrm{i}}) + 0.32p, \quad (1)$$

which has been derived from 20th century earthquakes in the Middle East with recalculated surface wave magnitude from the Prague formula (Ambraseys 1992). Intensities I_{i}, are on the Medvedev–Sponheuer–Karnik (MSK) scale, and distances r_{i} (in km) in the near-field are either site-source distances or distances from the closest point of the causative fault rupture. In the far-field r_{i} is the average radius of the isoseismal of intensity I_{i}, which was calculated using the 'kriging' technique (Olea 1999), a contouring method employed successfully for earthquakes in other parts of the Middle East (Ambraseys & Douglas 2004). In eq. (1), which is valid for Ii < VIII, p is 0 for mean value and 1 for 84 percentile. Fig. 2 shows eq. (1) as a function of distance and intensity I_{i}.

For the assessment of seismic hazard in the region of the Dead Sea Fault Zone, eq. (1) was recalibrated using 20th century earthquakes within a smaller region, defined by 32° to 38°N and 34°E to 40°E. This area includes all the major constituent tectonic elements of the Dead Sea Fault Zone and of the active zones adjacent to it, such as its junction with the southeast Anatolian Fault, the little understood off-shore fault system, which is located between the eastern Mediterranean coast and Cyprus in the west, as well as with the Palmyra structures in the east. It includes southeastern Turkey, the whole of Cyprus, Syria, Lebanon, Israel, Jordan, the westernmost part of Iraq and parts of northeastern Egypt and Saudi Arabia.

The fitted equation to the available intensity I_{i}, distance r_{i}, and magnitude M_{S} data is

$$M_{\mathrm{SCi}} = -0.138 + 0.554(I_{\mathrm{i}}) + 0.0033(r_{\mathrm{i}}) + 1.54\log(r_{\mathrm{i}}) + 0.31p, \quad (2)$$

similar to eq. (1). For distances greater than *ca.* 70 km eq. (2) overestimates M by up to 0.4 M_{SCi} units, and underestimates M_{SCi} for greater distances by the same amount. Residuals are comparable with the standard deviation in the determination of M_{SCi}. Eq. (2) is presented in order to show the effect of regional variations on the scaling of magnitude relations, which are important in hazard assessment. For the sake of uniformity with previous studies eq. (1) was used.

Table 1. Parametric catalogue of earthquake of $M_S \geq 7.0$ in the regions of the Gulf of Corinth, Sea of Marmara and Dead Sea Zone.

G. Corinth	Marmara Sea						Dead Sea					
None	Y	M	D	N	E	M_S	Y	M	D	N	E	M_S
	32	00	00	40.5	30.4	7.0	363	5	19	31.5	35.4	7.4
	68	00	00	40.7	30.0	7.2	551	7	9	33.9	35.9	7.3
	121	00	00	40.5	30.1	7.4	746	1	18	32.8	35.8	7.0
	123	11	10	40.3	27.7	7.0	860	1		35.5	35.5	7.0
	160	00	00	40.0	27.5	7.1	1157	8	12	35.3	36.4	7.2
	180	05	03	40.6	30.6	7.3	1170	6	29	34.7	36.4	7.3
	268	00	00	40.7	29.9	7.3	1202	5	20	34.1	36.1	7.2
	358	08	24	40.7	30.2	7.4	1212	5	1	30.0	35.0	7.0
	447	11	06	40.7	30.3	7.2	1458	11	16	31.0	35.3	7.1
	478	09	25	40.7	29.8	7.3	1588	1	4	29.0	36.0	7.2
	484	00	00	40.5	26.6	7.2	1759	11	25	33.7	35.9	7.5
	740	10	26	40.7	28.7	7.1	1822	8	13	36.7	36.8	7.4
	989	10	25	40.8	28.7	7.2	1837	1	1	33.3	35.5	7.0
	1063	09	23	40.8	27.4	7.4	1872	4	3	36.4	36.5	7.0
	1296	06	01	40.5	30.5	7.0						
	1343	10	18	40.9	28.0	7.0						
	1354	03	01	40.7	27.0	7.4						
	1419	03	15	40.4	29.3	7.2						
	1509	09	10	40.9	28.7	7.2						
	1556	05	10	40.6	28.0	7.2						
	1625	05	18	40.3	26.0	7.1						
	1659	02	17	40.5	26.4	7.2						
	1672	02	14	39.5	26.0	7.0						
	1719	05	25	40.7	29.8	7.4						
	1737	03	06	40.0	27.0	7.0						
	1766	05	22	40.8	29.0	7.1						
	1766	08	05	40.6	27.0	7.4						
	1855	02	28	40.1	28.6	7.1						
	1894	07	10	40.7	29.6	7.3						
	1912	08	09	40.8	27.2	7.3						
	1953	03	18	39.9	27.4	7.1						
	1957	05	26	40.7	31.0	7.2						
	1967	07	22	40.7	30.7	7.2						
	1999	08	17	40.8	30.0	7.4						

Table 2. Conspectus of data used in the study.

	Gulf of Corinth		Marmara Sea Region		Dead Sea Fault	
	1703–1995	1900–1995	1.−2000	1900–2000	100–2000	1900–2000
Period examined	37.5–38.5	37.5–38.5	39.5–41.5N	39.5–41.5N	29.0–37.0N	29.0–37.0N
Region defined by its corner coordinates	varies	varies	26.0–31.0E	26.0–31.0E	varies	varies
Length of the region (km)	135	135	420	420	880	880
Width of the region (km)	80	80	220	220	200	200
Surface area ($\times 104$) km^2	1.2	1.2	9.2	9.2	16	16
Predominant style of faulting	N	N	RL	RL	LL	LL
Average seismogenic thickness (km)	10	10	10	10	10	10
Total number of events identified	280	221	937	566	540	
Calculated event M_S	175	151	553	445	139	59
Number of events $M_S > 5.0$	73	49	176	75	82	15
Number of events $M_S > 6.0$	36	13	82	16	38	1
Number of events $M_S > 6.8$	2	0	52	8	21	0
Standard deviation of single observed M_S	0.35	0.2	0.35	0.2	0.35	0.25
Standard deviation of event M_S	0.17	0.07	0.15	0.05	0.2	0.1
Min. and Max. M_S used to assess velocity	6.0 6.8		6.8–7.4		6.8–7.5	
Mo contribution from smaller events	1.3		1.7		1.6	

Errors in M_S

The usual procedure for the estimation of magnitude is that for a given historical earthquake, M_{SCi} is calculated with eq. (1) from as may sitesource distances or isoseismal radii as are available and the average value of M_{SCi} is the event magnitude M_S.

It has been found that for historical earthquakes in the eastern Mediterranean the average standard deviation of a single M_{Si}

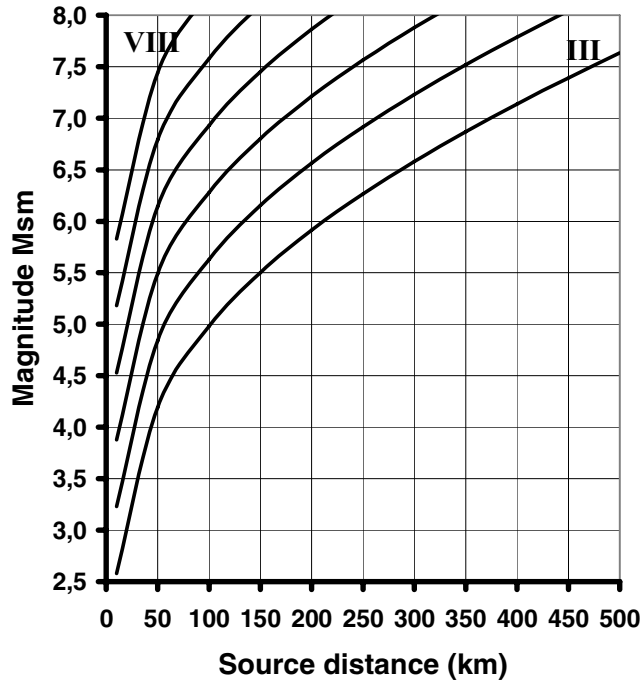

Figure 2. Plot of macroseismic magnitude M_{Sm} from eq. (1) for intensities I_{i} = III to VIII (MSK) scale with source distance r_{i} (in km). In the near-field, r_{i} are site-source distances or site distances from the closest point of the causative fault rupture.

determination σ_S is usually 0.4–0.5 M_{S} units, while the average standard deviation of the mean event magnitude σ varies between 0.15 and 0.30 M_{S} units. For events reported from very few places this value can be larger. As is to be expected in certain cases, the paucity of data may contribute a rather large uncertainty in the assessment of M_{S} with no foreseeable possibility of reducing it.

For the instrumental period, after 1912, the standard deviation of station magnitudes σ_{S} remains nearly constant for the whole 100-yr-long period, with a mean value of ± 0.25 M_{S} units but with considerable scatter (± 0.09). The standard deviation of the mean $\boldsymbol{\sigma}$ varies somewhat with magnitude and is on average ± 0.10 in M_{S} units (± 0.05) (Ambraseys & Douglas 2000).

Seismic moments

Regarding seismic moments, for more recent earthquakes Mo values are either Harvard CMT estimates or calculated from P/SH modelling, taken from published sources.

For historical earthquakes or for events for which M_0 is not available, seismic moments were estimated from surface wave magnitudes using the bilinear 'regional' relation, derived specifically for the eastern Mediterranean and the Middle East (Ambraseys & Jackson 2000).

The 'global' $\log(M_0)$–M_{S} relations of Ekström and Dziewonski (1988) and Ekström's for 'continental' earthquakes (Ekström 1987) were also used for comparison.

The 'continental' relation yields the smallest Mo values for a given $M_{\mathrm{S}} > 6.0$, while the 'regional' relation yields M_0 values much closer to CMT estimates, which are about 20 per cent smaller than those from the 'global' relation.

Frequency–magnitude distribution

For short-term observations, regional seismicity is well described by Gutenberg's cumulative frequency–magnitude relation

$$\log(\mathrm{N/y.a}) = \alpha - \beta M_{\mathrm{S}}, \tag{3}$$

in which (N/y.a) is the annual number of earthquakes of magnitude equal to, or greater than, M_{S} per unit area (a). However, as can be demonstrated along a fault zone, the same type of distribution is not proper for the description of seismicity over a long period of time.

Contribution of small earthquakes to the total moment

For the assessment of slip rates, data sets need to be as complete as possible in terms of magnitude. However, in long-term seismicity studies the data is necessarily incomplete and restricted to the larger events, usually of magnitudes greater than 6.0.

Therefore, the calculation of total moment release M_0^{T} requires the addition to the known total moment of the contribution from smaller magnitudes not accounted for in the summation. This depends on the range of M_{S} over which the moments are explicitly summed, as well as the likely size of the largest earthquake. It depends also on the exponent β (M) in the frequency–magnitude relation, which may be the linear, piecewise linear, or, at large M_{S} values, non-linear. It also depends on the choice of the scaling $\log(M_0)$–M_{S} law, (e.g. Molnar 1979; Ambraseys & Sarma 1999). M_0^{T} may be expressed as $M_0^{\mathrm{T}} = q(M_0^{\mathrm{M}})$, in which M_0^{M} is the known sum of moments calculated from the available magnitude range and scaling law.

Variation of slip rate with time

The seismic moments of the earthquakes were summed to obtain estimates of the variation of shear or extensional velocity with time for 300, 1900 and 2000 yr periods of observations using

$$u(t) = [(T)(H)(L)(\mu)]^{-1} \sum_{0}^{\mathrm{T}} (M_0), \tag{4}$$

where M_0 (dyn cm) are the seismic moments of individual events during a period of observation of T years; H is the seismogenic thickness for strike-slip faults or the width for normal faults; μ is the rigidity (3.0×10^{11} dyn cm^2) and L is the length of the fault zone. It is assumed that each event contributes to this motion and used throughout an average seismogenic thickness of 10 km, regardless of actual crustal depths known in the region.

It is possible that some of the smaller events in these three regions may have had fault mechanisms different from the predominant mechanism in the region, but this assumption is not thought to be an important source of error.

Note that the average slip rate is not representative of the average long-term velocity for periods of observation, which are too short to exhibit the repeat time of the larger earthquakes.

GULF OF CORINTH

The Gulf of Corinth is 135 km long and 80 km wide with an equivalent surface area of 1.2 square degrees, located in a region of crustal extension, which is bounded on both sides by normal faults Fig. 1.

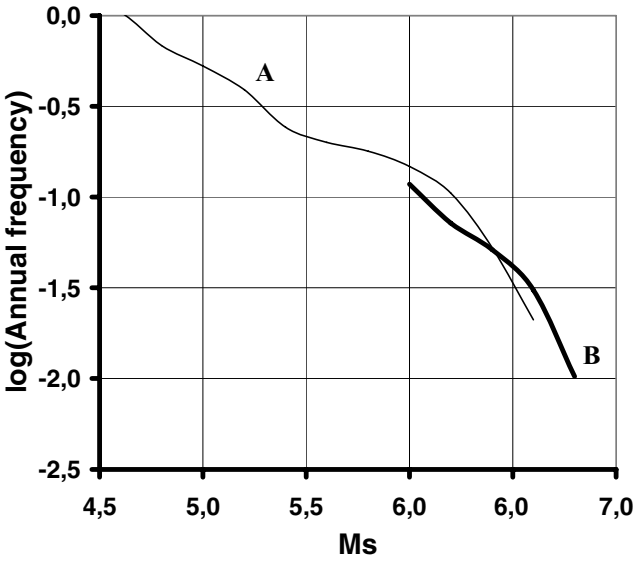

Figure 3. Annual frequency distribution per square degree for the region of the Gulf of Corinth. Thick line (B) is for the period 1703–2000, and thin line (A) for the 20th century.

Seismicity

Over the 300 yr period since 1700, for which macroseismic information is available, the seismicity of the Gulf region appears to have been relatively high with none of the events, however, exceeding M_S of about 6.7.

The historical and instrumental records for this 300 yr period consist of more than 200 earthquakes, for 175 of which it was possible to assess macroseismic or instrumental magnitudes for the estimate of extensional velocities. The data set seems to be complete for events within a rather narrow M_S range, 6.0–6.8. For smaller events incompleteness is partly due to fact that there are as many earthquakes with epicentral areas on land as in the Gulf, which does not allow the assessment of the macroseismic magnitudes.

Annual frequency distribution

Fig. 3 shows the short-term annual frequency–magnitude distribution, normalized to a square degree, for the period 1900–1995, which is relatively complete down to about $M_S = 4.5$, showing a reasonable β value of -0.6. Also shown for comparison is the long-term frequency distribution for the period 1703–1900, of events in the narrow magnitude range 6.0–6.8.

It has been observed that at the upper end of M_S the two curves tend to coalesce and that the slope of the latter curve, which may be considered to be an extension of the former, steepens from $\beta = -0.6$, tending asymptotically to $\beta = -1.4$, suggesting an upper bound for M_S. This lack of earthquakes greater than M_S 6.7 probably reflects the lack of continuity of faults, with few fault segments in Central Greece being demonstrably continuous for more than about 20–25 km, which is consistent with M_S 6.7.

Velocities

The time variation of extensional velocities is shown in Fig. 4 for a seismogenic thickness of 10 km.

The irregular rates in the first 100 yr of the record are partly due to the short time intervals used to calculate velocities at the beginning of the historical period. For longer time intervals, and for the remaining 250 yr, the velocity is stable, suggesting that 300 yr is sufficiently long to estimate an average moment release rate for this part of Greece and an average extension rate across the Gulf of Corinth of 1.38 cm yr^{-1}. Similar rates have been documented for a larger region (twice as long and wide).

Direct velocity measurements

These extensional velocities are similar to the geodetically estimated extension velocities. Clark *et al.* (1997) estimated 1.0 cm yr^{-1} N–S extension in the western Gulf and 0.4 cm yr^{-1} in the eastern Gulf, averaged over a 100 yr period by re-occupying first order triangulation points with Global Positioning Systems (GPS), and similar values of 1.3 cm yr^{-1} and 0.6 cm yr^{-1}, averaged over a 5 yr period with GPS alone.

Agatza-Balodimou *et al.* (1995) obtained a higher average extensional rate of about 1.8 cm yr^{-1} over a 20 yr period from a re-occupation of lower order, and less accurate, triangulation points with GPS. Thus for the Gulf of Corinth, although seismicity alone cannot resolve the difference in extension rate between the eastern and western Gulf, it does indicate that the likely velocity across the Gulf of Corinth should be 1.4 cm yr^{-1}. Given the errors, this estimate is almost the same as that calculated from GPS and triangulation surveys of a much larger area that includes the adjacent

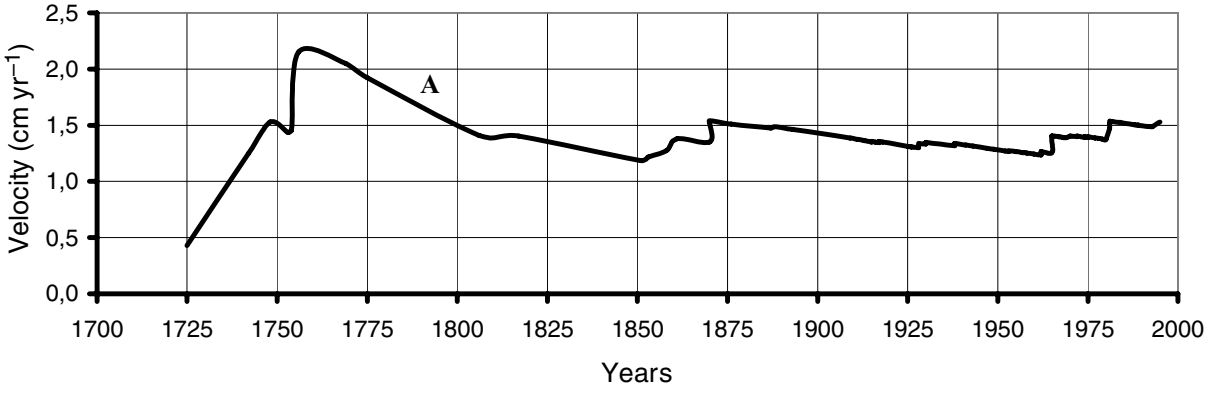

Figure 4. Average velocity of the Gulf of Corinth during the period 1703 to 200 calculated from eq. (4) for the regional $\log(M_0)$–M_S relation. H is the assumed seismogenic thickness of 10 km, and L is the length of the fault zone. Note that for periods T (yr) which are too short to disclose the repeat time of the larger earthquakes average slip rates (A), are not representative of the long term velocity.

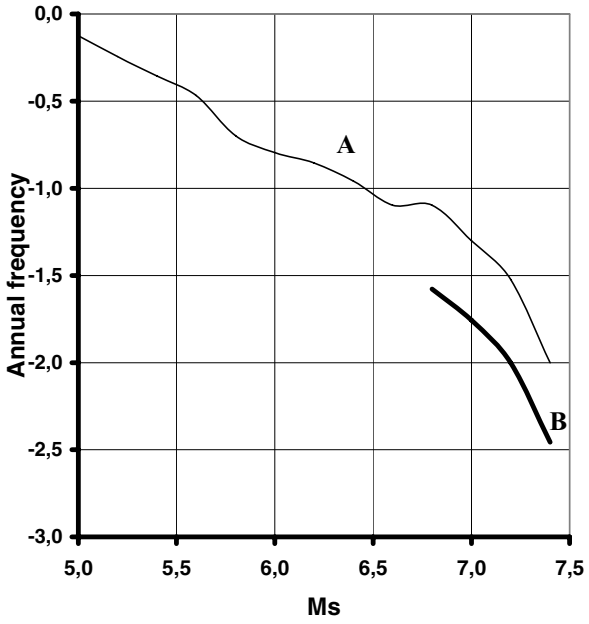

Figure 5. Annual frequency distribution per square degree for the region of the Sea of Marmara. Thick line (B) is for the period 1–2000, and thin line (A) for the 20th century.

Gulf of Evia, which shows a combined velocity of only 1.2 cm yr^{-1} (Jackson 1999). See also Avallone *et al.* (2004) seen very recently, after this article was written.

MARMARA SEA REGION

Another region with a much longer and better-recorded seismic history is the region of the Sea of Marmara in north-western Turkey, which is roughly bounded by 39.5°N to 41.5°N and 26°E to 31°E.

Tectonics

The region is dominated by the right-lateral North Anatolian Fault Zone, which accommodates most of the westward motion of Turkey, a narrow and localized character, clearly defined by the predominantly strike-slip surface along its entire 1000 km length, associated with a series of major earthquakes.

The Marmara submarine fault system is the result of oblique extension and as such is segmented showing asymmetric slip partitioning, with the faults that bound the north of the basin carrying more strike-slip motion than predicted from the Anatolia–Eurasia plate motion, and faults to the south having a perpendicular component (Armijo *et al.* 2002; Flerit *et al.* 2003).

Seismicity

The revised seismicity of the region over the last 2000 yr shows no evidence for truly large earthquakes of a size comparable to that further east in the North Anatolian Fault Zone. Events are smaller, in keeping with the known fault segmentation of the Basin.

Annual frequency distribution

Fig. 5 shows the annual frequency–magnitude distribution per square degree for the region, derived from 20th century data. For $M_S < 6.5$ the distribution follows eq. (3) with a β value of about -0.7, which for larger magnitudes dips to much smaller β values.

If the period of observations is extended to about 2000 yr it may be observed that the larger magnitudes, at the upper end of the recurrence curve, because the 20th century record is too short to disclose the repeat time of larger earthquakes, the relation shows an asymptotic behaviour suggesting a genuine departure from Gutenberg's eq. (3).

The implication is that large earthquakes in the Marmara region are less frequent when assessed from the long-term data set than from the usual 100 yr instrumental period, making the notion of a recurrence time, in its usual definition, and of hazard assessment, questionable.

Variation of slip rate with time

The variation with time of slip rates is shown in Fig. 6, again for a seismogenic thickness of 10 km. If it is assumed that the typical thickness or locking depth is smaller, say 7 km (Meade *et al.* 2002), this would increase the velocity by almost 40 per cent.

With the exception of the irregularity of the velocity in the first centuries, the velocity for the rest of the period is quite constant with an average value of 2.0 ± 0.4 cm yr^{-1}.

The time interval between the first year and the year beyond which the average slip rate becomes stable, may be a measure of the length of the repeat time between large events. However, confirmation of

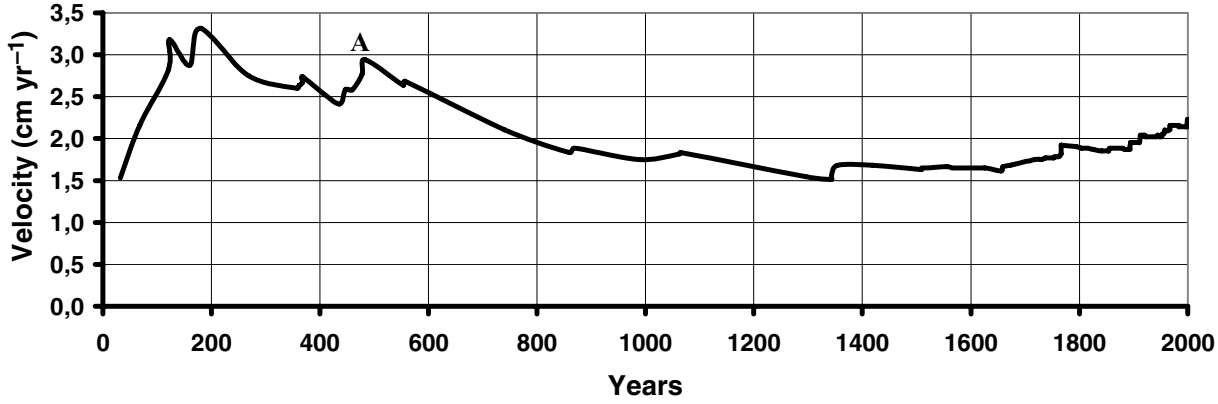

Figure 6. Variation of velocity of the region of the Sea of Marmara during the period 1–2000 calculated from the regional $\log(M_0)$–M_S relation (see caption Fig. 4).

this would require the study of a much larger area over a longer period of time, which, at present, is not feasible.

Meade has shown that the northern straight strand of the North Anatolian Fault in the Marmara Basin carries four times as much right-lateral motion as does the southern strand (Meade *et al.* 2002). Historical seismicity cannot confirm this or the hypothesis of a single, through going, purely strike-slip fault (Le Pichon *et al.* 2001).

It does confirm, however, that the slip rate and the moment release along this straight fault geometry over the last 2000 yr accounts for the known right-lateral shear velocity across the Marmara region observed by GPS. There is no evidence for truly large earthquakes of a size comparable to those in the North Anatolian Fault Zone, earthquakes here being smaller, in keeping with the known fault segmentation of the Basin.

Measured slip rate

Slip rates from GPS measurements show values between 2.2 and 2.6 ± 0.3 cm yr^{-1} (Straub 1996; Reilinger *et al.* 1997) and correspond to the elastic strain to be accounted for by future earthquakes and seismic creep (Walcott 1984).

DEAD SEA FAULT ZONE

The third region investigated is that of the Dead Sea Fault Zone, which extends for 880 km, from 28°N in the south, to 36°N in the north, where it merges with the East Anatolian Fault Zone and which has an equally long, but far less well recorded seismic history, than the Marmara Sea region, Fig. 1.

The region

In defining the study region allowance was made for uncertainties in the location of historical earthquakes that are likely to be associated with the fault zone. The width for this zone was assumed to be 100 km, although activity may spread out more than this in restraining bends, such as those associated with the Yammouneh fault, the Palmyrides, and the East Anatolian Fault Zone. All earthquakes located within this zone were considered as candidates for such an association.

Tectonics

The northward motion of Africa relative to Eurasia is described by a rotation and an average motion of about 0.6 cm yr^{-1}. Arabia moves northwards faster than this because its motion is enhanced by seafloor spreading in the Red Sea. It is this effect that causes the left-lateral strike motion on the Dead Sea Fault System, which extends from the Gulf of Aqaba in the south to SE Turkey in the north.

The Dead Sea Fault system consists of left-lateral fault segments that connect the active oceanic spreading centres in the Red Sea to the compressional deformation zones in southern Anatolia and the Zagros (Garfunkel *et al.* 1981). It has a total length of about 900 km, and includes several pull-apart basins (such as the Dead Sea Basin) and push-up zones, formed in regions of overlap between left-stepping and right-stepping fault segments, respectively.

In common with all major continental strike-slip faults, the Dead Sea fault system is segmented, with rupture in individual earthquakes limited in length by structural discontinuities or bends.

However, if the interpretation by McClusky *et al.* (2003) is correct, it implies that the Turkey–Africa boundary, running south of Cyprus is on the African plate. This would require significant left-lateral slip on the northern part of the Dead Sea Fault Zone, in contrast to the interpretation of Butler *et al.* (1997, 1998) who suggest that the Africa–Arabia boundary follows the offshore Roum fault south of Beirut.

The straightness of the Yammouneh fault segment suggests that it is pure strike-slip in character and that it does not accommodate the necessary shortening component required by its orientation: this component will be taken up on nearby thrusts that will also pose a seismic hazard. However, because of the oblique orientation of the Yammouneh fault, relative to the Arabia–Africa slip vector, it is extremely likely that other faults (possibly including the Roum fault) are active between 31°N and 35°N.

In addition, not all the strike-slip component may be restricted to the Yammouneh fault, and other adjacent or nearby faults, such as the Roum fault, may also be participating in the slip of the fault zone, with other fault segments being longer, moving in less frequent, but larger earthquakes. Other adjacent faults, in the same region are also capable of producing earthquakes, but how significant these are is difficult to say.

As for the seismic activity, which occurs offshore between Beirut and Cyprus, there is considerable historical evidence of earthquakes, the size of which cannot be quantified.

Seismicity

The activity of the last 100 yr has been far lower than is necessary to account for the Arabia–Africa motion, yet in previous centuries large earthquakes are known to have occurred (Jackson & McKenzie 1988; Ambraseys & Melville 1988; Ambraseys & Barazangi 1989; Ambraseys & Jackson 1997).

The present day quiescence of the Dead Sea Fault Zone becomes apparent when considering that, excluding the earthquake of 1995 November 22 (M_S 7.1) on the extension of the fault zone in the Gulf of Aqaba in the south, only one earthquake of M_S 6.0 has occurred in the Dead Sea Fault Zone in the whole of the last century, namely, the earthquake of 1927 July 11 (M_S 6.0).

Very few focal mechanisms are available from the CMT catalogue and they are all for relatively small ($M_S < 5.7$) earthquakes. Most of them show the expected left-lateral motion parallel to the Dead Sea Fault Zone and are apparently good solutions. Others located in a region of complicated conjugate strike-slip faulting west of the Sea of Galilee, west of the Dead Sea fault, show focal mechanisms with nodal planes striking NE–SW and NW–SE rather than N–S (Ron *et al.* 1984). This is a useful reminder that not all earthquakes in the region occur on the main structure.

West of the Dead Sea Fault Zone around the Gulf of Iskenderun the available mechanisms show the NE–SW left-lateral motion associated with the East Anatolian fault system and also some extension, which is expected between Turkey and Africa in this area (Jackson & McKenzie 1984).

Some scattered activity occurs offshore between Lebanon and Cyprus, with a number of poorly located events of $M_S > 5.7$ before 1963, which seem to be deeper than normal.

Little is known of the geological structures offshore that accommodate the Africa–Turkey motion between Cyprus and the Gulf of Iskenderun. However, there is evidence that quite a few earthquakes of magnitude 6.0 or more did occur offshore in historical times.

The seismic activity of the last 2000 yr, however, is quite different. It is probable that at least two large earthquakes in 1202 and 1759 occurred on the straight Yammouneh fault segment of the main left-lateral fault system itself, which runs NNE–SSW for about

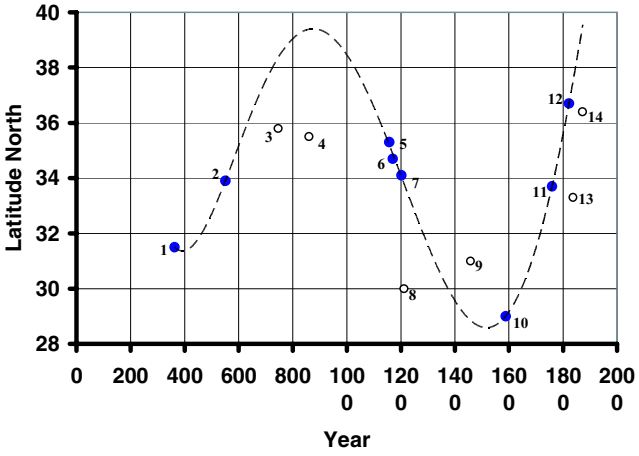

Figure 7. Scatter plot of the larger earthquakes in the Dead Sea Fault Zone since AD 363, showing a tendency to migrate with some regularity with time along the trend of the fault zone, first to the north, then to the south and again to the north. Curve shows the trend for events of $M_S \geq 7.2$. Open circles are for earthquakes $7.0 \leq M_S < 7.2$. Point labelling numbers refer to entries in Table 1.

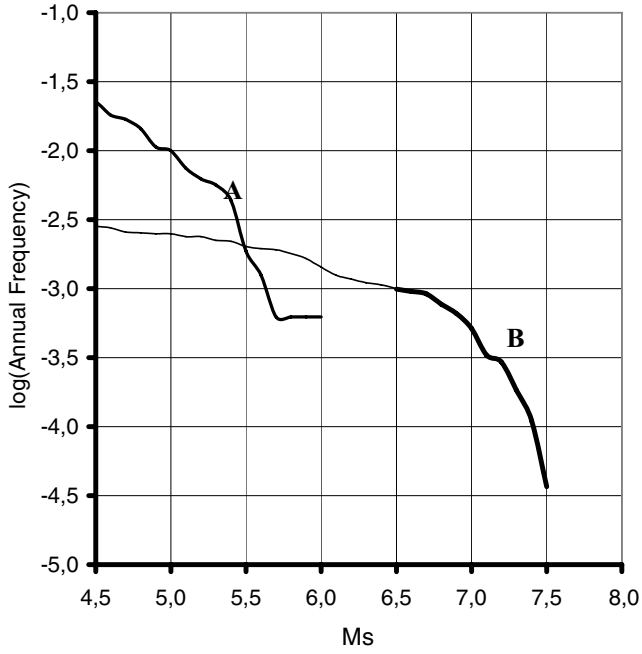

Figure 8. Annual frequency distribution of earthquakes per square degree in the Dead Sea region. Thick line (B) is for the period 1–2000, and thin line (A) for the 20th century.

150 km and is thus oblique to the overall Africa–Arabia motion. It is, therefore, not surprising that in this area the deformation is probably distributed over more than one fault, and may even be separated into its strike-slip and thrust components, as is seen elsewhere in regions of oblique convergence. A manifestation of this distributed deformation may be the large (M_S 7) earthquake of 1837 in southern Lebanon, which appears not to have occurred on the Yammouneh fault, and may have been on the Roum fault instead.

The available historical data suggests that both the 1202 and 1759 earthquakes ruptured the Yammouneh fault over a distance of about 100 km, which covers most of its length between the more N–S trending segments of the fault system to the north and south.

An observation about the activity along the Dead Sea Fault Zone is the 2000-yr-long regularity with which larger earthquakes ($M_S > 7.0$) migrate with time. A scatter plot of the larger earthquakes in the Dead Sea Fault Zone since AD 363, which are shown in Table 2 and Fig. 7, shows that there is a tendency for the location of events to migrate with time along the trend of the fault zone, first to the north, then to the south and again to the north, with a surprising regularity.

The reason for this too neat pattern is not understood, and cannot be explained without proper knowledge of the long-term seismicity associated with the interaction of the Dead Sea Fault Zone with the adjacent East Anatolian Fault Zone in the north. Earthquakes north of 37°N have not been included and large earthquakes rupture a considerable length of the fault, so that their representation as a point may work well to make a graph like this and may obscure what is in reality a much more complex situation.

Annual frequency distribution

The annual frequency–magnitude distributions per square degree from the 100 yr long data set, is shown in Fig. 8. It follows eq. (3) only up to $M_S = 5.4$, with a β value of about -0.8, which suggests that a period of observations of 100 yr is too short for the Dead Sea Fault Zone to exhibit its long-term seismic potential.

This lack of larger magnitudes become apparent from the fact that the average slip velocity during the 20th century hardly exceeds one tenth of the average slip velocities based on reliable GPS measurements.

How much more active the Dead Sea Fault Zone was in the past can be seen from the entries in the magnitude column of Table 2, where of the 14 significant earthquakes during the last 20 centuries, none occurred in the 20th century.

An impression of the seismic potential of the fault zone can be formed, however, from the frequency distribution of earthquakes over the much longer period of 2000 yr, shown in Fig. 7. This figure confirms that the actual frequency–magnitude distribution can be extended to larger magnitudes at which the distribution becomes smoothly asymptotic to M_S about 7.5.

Variation of slip rate with time

The time variation of slip velocity of the Dead Sea Fault Zone for a seismogenic thickness of 10 km is shown in Fig. 9.

The average slip rate is 0.35 ± 0.08 cm yr^{-1} and the general slip pattern suggests that different segments of the main Dead Sea Fault system remain locked between slip events in major earthquakes, which are responsible for sharp velocity changes.

For the Dead Sea Fault Zone the main conclusion is that the most likely overall slip rate across the zone is about 0.35 cm yr^{-1}, and that earthquake activity of the 20th century is definitely not a reliable guide to the activity over a longer period.

Estimates of rates from measurements

Several early plate models that specifically address this region and which are based on re-interpretations of the seafloor, earthquake and fault data have been proposed (Joffe & Garfunkel 1987; Le Pichon & Gaulier 1988; Jestin *et al.* 1994). All of them predict about 0.8–1.0 cm yr^{-1} of nearly N–S left-lateral slip across the Dead Sea Fault Zone as a whole, which is now known to be an overestimation.

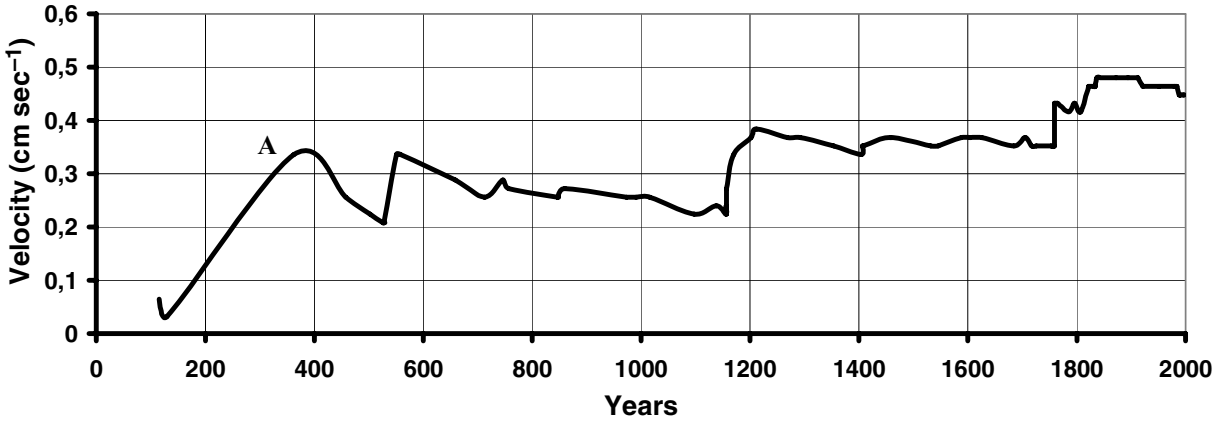

Figure 9. Variation of average velocity of the Dead Sea Fault Zone for the period 100–2000, calculated from the regional $\log(M_0)$–M_S relation, plotted on a velocity scale five times larger than in Figs 3 and 6 (see caption Fig. 4).

From the earthquake distribution and known patterns of active faulting, the motion is likely to be confined to a relatively narrow zone perhaps 100 km wide, but may spread out more that this in restraining bends, such as those associated with the Yammouneh fault and the Palmyrides (McBride *et al.* 1990; Chaimov *et al.* 1992; Butler *et al.* 1998).

Rates of movement are known from global plate models, GPS measurements and field observations, but not in great detail, so that no attempt is made here to synthesize them. The new Arabia–Africa Euler pole calculated from GPS measurements, predicts plate motions from 0.4 to 0.5 cm yr^{-1} along the southern Dead Sea Fault, to about 0.6 to 0.7 cm yr^{-1} along the northern Dead Sea Fault (McClusky *et al.* 2003), while the local GPS survey for the central Dead Sea Fault gives only 0.26 cm yr^{-1} (Per'eri *et al.* 1998).

Elastic dislocation modelling of GPS data in Israel yields a velocity of about 0.3–0.4 cm yr^{-1} Wdowinski *et al.* (2004). Also for the central part of the fault zone, GPS-based models give 0.4 at latitude of 32°N, and 0.5 cm yr^{-1} at a latitude 34°N (Sella *et al.* 2002). Further to the north, at latitude about 36°N, a GPS-based model gave 0.6 cm yr^{-1} (McClusky *et al.* 2003) or 0.8 cm yr^{-1}, as found by Sella *et al.* (2002).

A few field measurements between the Dead Sea and the Gulf of Aqaba, based on Late Pleistocene faulted alluvial fans give a slip rate between 0.2 and 0.6 cm yr^{-1}, (Klinger *et al.* 2000). Also, in the north end of the Gulf of Aqaba, in Wadi Araba, Early Pleistocene drainage reconstruction of displaced alluvial terraces predicts similar velocities and 0.3 and 0.75 cm yr^{-1} (Ginat *et al.* 1998). Further north, south of the Dead Sea, offset stream channels and fan surfaces suggest 0.47 mm yr^{-1} (Niemi *et al.* 2001), while in the central part of the Dead Sea Fault, along the 100 km long Serghaya fault, field observations of Mid to Late Holocene channel displacements made by (2003) give velocities of 0.13–0.15 cm yr^{-1}. Within the same part of the fault zone, displacements of Late Pleistocene/Early Holocene fans on the Yammouneh fault show values of 0.4–0.5 cm yr^{-1}, (Gomez, private communication, 2005). The same model at latitude 34°N, gives 0.58 cm yr^{-1}, and at latitude 32°N gives 0.67 cm yr^{-1}. Finally, at latitude 35°N the displacement of the foundations of a 2000-yr-old Roman aqueduct on the Massyaf fault segment, based on Mid to Late Holocene channel, suggests a slip rate of 0.69 cm yr^{-1}. (Meghraoui *et al.* 2003).

The current interpretation of the GPS data suggests that an average rate of about 0.45 cm yr^{-1} $\pm$ 0.2 applies to the entire length of the zone between Aqaba and Antakya, perhaps somewhat larger in the north and smaller in the south, and that a proportion of the Arabia–Africa motion may continue offshore south of Beirut along the Roum fault.

Again here, historical seismicity alone cannot resolve the difference in slip rate between the north and south Dead Sea Fault Zone.

DISCUSSION AND CONCLUSIONS

The objective of this study was to understand better the current tectonic activity and seismic hazard of three regions in the Eastern Mediterranean by extending the period of the 20th century macroseismic observation by a factor of 20.

As it is not possible to know what will happen in the future, in order to estimate likely earthquake hazards it is necessary to find out what happened in the past and extrapolate from there.

In the process of doing this the level of uncertainty of the location of large historical earthquakes has been found to be good enough to guide field studies for further investigation of regional tectonics.

In some cases magnitudes are approximate and several factors could change these. Given the uncertainties in the original M_S values, the missing and unaccounted for seismic moment from subevents, the uncertainties in the depth and in the $\log(M_0)$–M_S scaling law, it is difficult to estimate more realistic velocities from historical seismicity alone. Arguing that the seismogenic thickness for some of the earthquakes is as much as 15 km, would reduce the velocities by a third.

Also, uncertainties in slip rates calculated from long-term historical data are relatively large, but in well-documented regions they are comparable to those calculated from field observations and GPS. In view of all these uncertainties, it is surprising that estimates from historical data are almost the same as those calculated from GPS and triangulation surveys.

We find that the major portion, perhaps effectively all of the long-term motion in the three regions studied, including that due to missing events, is probably achieved by seismic slip on faults, and that aseismic creep may be relatively unimportant. However, the uncertainties in slip rates are large enough to mask likely differences that may exist in various parts of a region, and answers to the problem of seismic *versus* aseismic slip might well come from geodetic observations.

It has been calculated that the size of little known historical earthquakes can be better quantified by constraining their magnitude within limits which satisfy regional mobility. This in turn, allows

the estimation of a more reliable long-term hazard model, and also the estimation of slip rates in regions for which GPS measurements are not available.

A by-product of the present work which concerns chiefly engineering seismology, is that in hazard modelling from short-term, 100-yr-long data sets, it is simply not reasonable to ignore the chance that much, or all, of the records may be from quiescent or energetic periods in seismic activity, particularly for small probabilities of exceedence. This is one of the possibilities that must be borne in mind when making assumptions with short-term data sets, and the principal reason why statistics alone cannot quickly and simply answer the question of seismic hazard evaluation.

This new information is consistent with what is known about earthquake mechanics today and it contributes to a better understanding of earthquake hazard.

ACKNOWLEDGMENTS

This work was supported by the project Archeoseismology and Paleoseismology for the Protection of Cultural Heritage and Archaeological Sites in the Middle East (APAME), headed by Prof. M. Meghraoui and sponsored by the European Commission, DGXII (ICA3-CT-2002-10024).

REFERENCES

Agatza-Balodimou, A., Briol, P., Lyon-Caen, H., 1995. 'Recent developments in deformation studies from geodetic data in the Corinthian Gulf', *Proc. 1st Intern. Symp. On Deformation in Turkey*, Publ. TMMOB-HMO, Ankara, pp. 758–769.

Ambraseys, N., 1992. Soil mechanics and engineering seismology, *Proc. 2nd Natl. Conf. on Geotech. Eng.*, (invited paper), Thessaloniki.

Ambraseys, N., 2002. The seismic activity of the Marmara Sea region over the last 2000 years, *Bull. seism. Soc. Am.,* **92,** 1–18.

Ambraseys, N.N. & Melville, C., 1988. An analysis of the eastern Mediterranean earthquake of 20 May 1202, in *Historical Seismograms and Earthquakes of the World*, pp. 181–200, ed. Lee, W., Academic Press, San Diego.

Ambraseys, N.N. & Barazangi, M., 1989. The 1759 earthquake in the Bekaa valley, *J. geophys. Res.,* **94,** 4007–4013.

Ambraseys, N. & Jackson, J.A., 1997. 'Seismicity and strain in the Gulf of Corinth (Greece) since 1694', *J. Earthq. Eng.,* **1,** 433–474.

Ambraseys, N. & Sarma, S., 1999. 'The assessment of total seismic moment', *J. Earthq. Eng.,* **3,** 439–46.

Ambraseys, N. & Douglas, J., 2000. Reappraisal of surface wave magnitudes in the eastern Mediterranean region and the Middle East, *Geophys. J. Int.,* **141,** 357–373.

Ambraseys, N. & Jackson, J., 2000. Seismicity of the Sea of Marmara (Turkey) since 1500, *Geophys. J. Int.,* **141,** F1–F6.

Ambraseys, N. & Douglas, J., 2004. Magnitude calibration of north Indian earthquakes, *Geophys. J. Int.,* **159,** 165–206.

Armijo, R. *et al.,* 2005. Submarine fault scarps in the Sea of Marmara pull-apart North Anatolian Fault: Implications for seismic hazard in Istanbul, *Geochem. Geophys. Geosyst.,* **6,** Q06009, doi:10.1029/2004GC000896.

Armijo, R., Meyer, B., Navarro, S., King, G. & Barka, A., 2002. Asymmetric slip partitioning in the Sea of Marmara pull-apart: a clue to propagation process of the North Anatolian Fault?, *Terra Nova,* **14,** 80–86.

Avallone, A. *et al.,* 2004. Analysis of eleven years of deformation measured by GPS in the Corinth Rift laboratory area, *Comptes Rendus Geosciences,* **336,** issues 4–5, March, 301–311.

Butler, R.W.H., Spencer, S. & Griffiths, H.M., 1997. Transcurrent fault activity on the Dead Sea transform in Lebanon and its implications for plate tectonics and seismic hazard, *J. geol. Soc. Lond.,* **154,** 757–760.

Butler, R.W.H., Spencer, S. & Griffiths, H.M., 1998. The structural response to evolving plate kinematics during transpression: evolution of the Lebanese restraining bend of the Dead Sea transform. in *Continental Transpressional and Transtensional Tectonics*, Vol. 135, pp. 81–106, eds Holdsworth, R.E., Strachan, R.A. & Dewey, J.F., Spec. Publ. Geol. Soc. Lond.

Chaimov, T.A., Barazangi, M., Al-Saad, D., Sawaf, T. & Gebran, A., 1992. Balanced cross sections and shortening in the Palmyride fold belt of Syria and implications for movement along the Dead Sea fault system, *Tectonics,* **9,** 1369–1386.

Clarke, P. *et al.,* 1997. Geodetic estimate of seismic hazard in the Gulf of Korinthos, *Geophys. Res. Lett.,* **24(11),** 1303–1306.

DeMets, C., Gordon, R.G., Argus, D.F. & Stein, S., 1994. Effect of recent revisions to the geomagnetic reversal time scale on estimates of current plate motions, *Geophys. Res. Lett.,* **21,** 2191–2194.

Ekström, G., 1987. A broad band method of earthquake analysis, *PhD thesis*, Harvard Univ., Cambridge, Massachusetts.

Ekström, G. & Dziewonski, A., 1988. Evidence for bias in estimation of earthquake size, *Nature,* **332,** 319–323.

Flerit, F., Armijo, R., King, G.C., Meyer, B. & Barka, A., 2003. Slip partitioning in the Sea of Marmara pull-apart determined from GPS velocity vectors, *Geophys. J. Int.,* **154,** 1–7.

Garfunkel, Z., Zak, I. & Freund, R., 1981. Active faulting in the Dead Sea Rift, *Tectonophysics,* **80,** 1–26.

Ginat, H., Enzel, Y. & Avni, Y., 1998. Translocated Plio-Pleistocene drainage systems along the Arava fault of the Dead Sea transform, *Tectonophysics,* **284,** 151–160.

Gomez, F. *et al.,* 2003. Holocene faulting and earthquake recurrence along the Segahya branch of the Dead Sea Fault System in Syria and Lebanon, *Geophys. J. Int.,* **153,** 658–674.

Hubert-Ferrari, A., Barka, A., Jacques, E., Nalbant, S., Meyer, B., Armijo, R., Tapponnier, P. & King, G., 2000. Seismic hazard in the Marmara Sea region following the 17 August 1999 Izmit earthquake, *Nature,* **404,** 269–273.

Jackson, J., 1999. Fault depth: a perspective from actively deforming regions, *J. Struct. Geol.,* **21,** 1003–1010.

Jackson, J. & McKenzie, D., 1984. Active tectonics of the Alpine-Himalayan belt between western Turkey and Pakistan, *Geophys. J. Roy. astr. Soc.,* **77,** 185–264.

Jackson, J.A. & McKenzie, D., 1988. The relationship between plate motions and seismic moment tensors and the rates of active deformation in the Mediterranean and the Middle East, *Geophys. J. R. astr. Soc.,* **93,** 45–73.

Jestin, F., Huchon, P. & Gaulier, J.M., 1994. The Somalia plate and the East African Rift system: present day kinematics, *Geophys, J. Int.,* **116,** 637–654.

Joffe, S. & Garfunkel, Z., 1987. Plate kinematics of the circum Red Sea—a re-evaluation, *Tectonophysics,* **141,** 5–22.

Klinger, Y., Avouac, J.P., Abu Karaki, N., Dobrath, L., Bourles, D. & Reyss, J.L., 2000. Slip rate on the Dead Sea transform fault in northern Araba valley (Jordan), *Geophys. J. Int.,* **142,** 755–768.

Le Pichon, X. & Gaulier, J.M., 1988. The rotation of Arabia and the Levant fault system, *Tectonophysics,* **153,** 271–294.

Le Pichon, X., Taymaz, T. & Sengör, C., 2000. Important problems to be solved in the Sea of Marmara, *Abstracts NATO Adv. Res. Seminar on Integration of Earth Sciences Research,* 66–67, Istanbul.

Le Pichon, X., Sengör, A.M., Demirbag, E., 2001. The active main Marmara fault, *Earth planet. Sci. Lett.,* **192,** 595–616.

Lyberis, N., Yurur, T., Chorowicz, J., Kasapoglu, E. & Gundogdu, N., 1992. The East Anatolian Fault: an oblique collisional belt, *Tectonophysics,* **204,** 1–15.

McBride, J.H., Barazangi, M., Best, J., Al-Saad, D., Sawaf, T., Al-Otri, M. & Gebran, A., 1990. Seismic reflection structure of intracratonic Palmyride fold-thrust belt and surrounding Arabian platform, *Syria. Am. Assoc. Petrol. Geol. Bull.,* **74,** 238–259.

McClusky, S., Reilinger, R., Mahmoud, S., Ben Sari, D. & Taelab, A., 2003. GPS constraints on Africa (Nubia) and Arabia plate motion, *Geophys. J. Int.,* **155,** 126–138.

Meade, B.J., Hager, B.H., McClusky, S.C., Reilinger, R., Ergintay, S., Lenk, O., Barka, A. & Ozener, H., 2002. Eatimates of seismic potential in the Marmara region from block models of secular deformation constrained by GPS measurements, *Bull. Seism. Soc.,* **92,** 208–215.

Meghraoui, M. *et al.*, 2003. Evidence for 830 years of seismic quiescence from palaeoseismology, archaeoseismology and historical seismicity along the Dead Sea Fault in Syria, *Earth planet. Sci. Lett.,* (in ICA3-CT2002-10024 Project, Strasbourg).

Meghraoui, M., 2004. Archaeoseismology and palaeoseismology for the protection of cultural heritage and archaeological sites in the Middle East, 2nd Year Report (2004–5)a, ICA3-CT2002-10024 Project, Strasbourg.

Meghraoui, M., 2005. Large earthquake faulting and implementation for the seismic hazard assessment in Europet RELIEF Project, 2nd Year Report (2004–5)b, EVG1-CT-2002-00069 Project, Strasbourg.

Molnar, P., 1979. Earthquake recurrence intervals and plate tectonics, *Bull. seism. Soc. Am.,* **69,** 115–133.

Niemi, T.M., Zhang, H., Atallah, M. & Harrison, J.B., 2001. Late Pleistocene and Holocene slip rate of the northern Wadi Araba fault, Dead Sea transform, *Jordan. Journal of Seismology,* **5,** 449–474.

Olea, R.A., 1999. *Geostatistics for Engineers and Earth Scientists*, Kluwer Acad. Pub. Dordrecht.

Parke, J., Minshull T., Anderson, G., White, R., McKenzie, D., Kuscu, I., Bull, J. & Sengor, A., 1999. Active faults in the Sea of Marmara, Western Turkey, imaged by seismic reflection profiles, *TerraNova,* **11,** 223–227.

Per'eri, S., Wdowoniski, S. & Shtivelman, A., 1998. Current plate motions across the Dead Sea fault as determined from 18 month of continuous GPS monitoring, Abstract, *26th Gen. Assembly European Seism. Commiss.,* Tel Aviv.

Reilinger, R., McClusky, S., Oral, M. *et al.*, 1997. Global Positioning System measurements of present-day crustal movements in the Arabia-Africa-Eurasia plate collision zone, *J. geophys. Res.,* **102,** 9983–9999.

Ron, H., Freund, R., Garfunkel, Z. & Nur, A., 1984. Block rotation by strike-slip faulting: structural and paleomagnetic evidence, *J. geophys. Res.,* **89,** 6256–6270.

Sella, G.F., Dixon, T.H. & Mao, A., 2002, REVEL: a model of Recent plate velocities from space geodesy, *J. geophys. Res.,* **107,** doi:10.1029/2000JB000033.

Scholz, C.H., Aviles, C. & Wesnousky, S., 1986. Scaling differences between large intraplate and interplate earthquakes, *Bull. seism. Soc. Am.,* **76,** 65–70.

Sigbjornsson, R. & Ambraseys, N., 2003. Uncertainty analysis of strong-motion and seismic hazard, *Bull. Earthq. Eng.,* **1,** 321–347.

Straub, C., 1996. Recent crustal deformation and strain accumulation in the Marmara Sea region, NW Anatolia, inferred from GPS measurements. *Mitteil. Inst. Geod. And Photogramm. ETH,* no. 58, Zurich.

Walcott, R.I., 1984. The kinematics of plate boundaries through New Zealand: a comparison of the short and long term deformation, *Geophys. J.,* **79,** 613–663.

Wdowinski, S. *et al.*, 2004. GPS measurements of currently crustal movements along the Dead Sea Fault, *J. geophys. Res.,* **109,** B05403.